Raman Spectra of Monolayer, Few-Layer, and Bulk $ReSe_2$: An Anisotropic Layered Semiconductor

Daniel Wolverson, Simon Crampin, Asieh S. Kazemi, Adelina Ilie, Simon J. Bending

Department of Physics, University of Bath, Bath BA2 7AY, UK

Supporting information

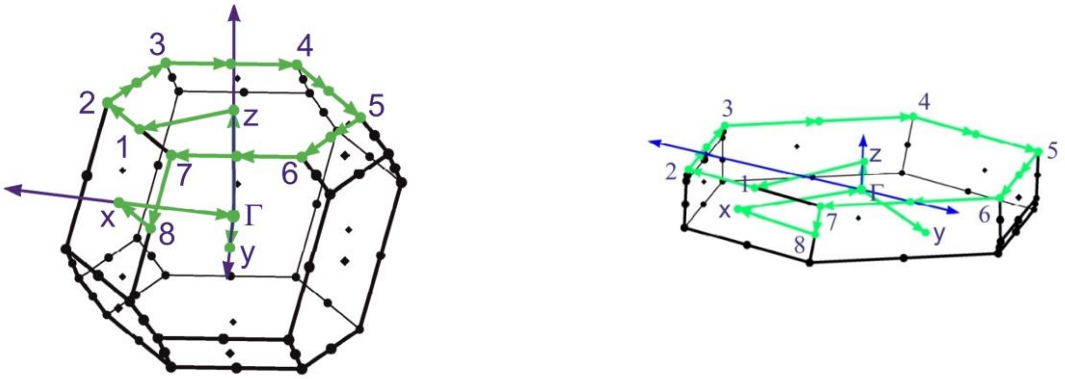

Figure 9. Left: the Brillouin zone of $ReSe_2$ showing the *k*-point paths used for the bulk 3D structure. Right: Brillouin zone of the quasi-2D structure used to model monolayer $ReSe_2$ in which the *c*-axis has been elongated by a factor of 5. The sequence of *k*-points is that used for the calculations shown in Figure 2 and, in both cases, starts from the Γ point, moves upwards to the central point of the near-hexagonal facet, circles that completely, and then moves down to the centre of one large facet, back to the Γ point, and then out to the centre of one more large facet. Figures generated using Xcrysden (Ref. 61 of the main text).

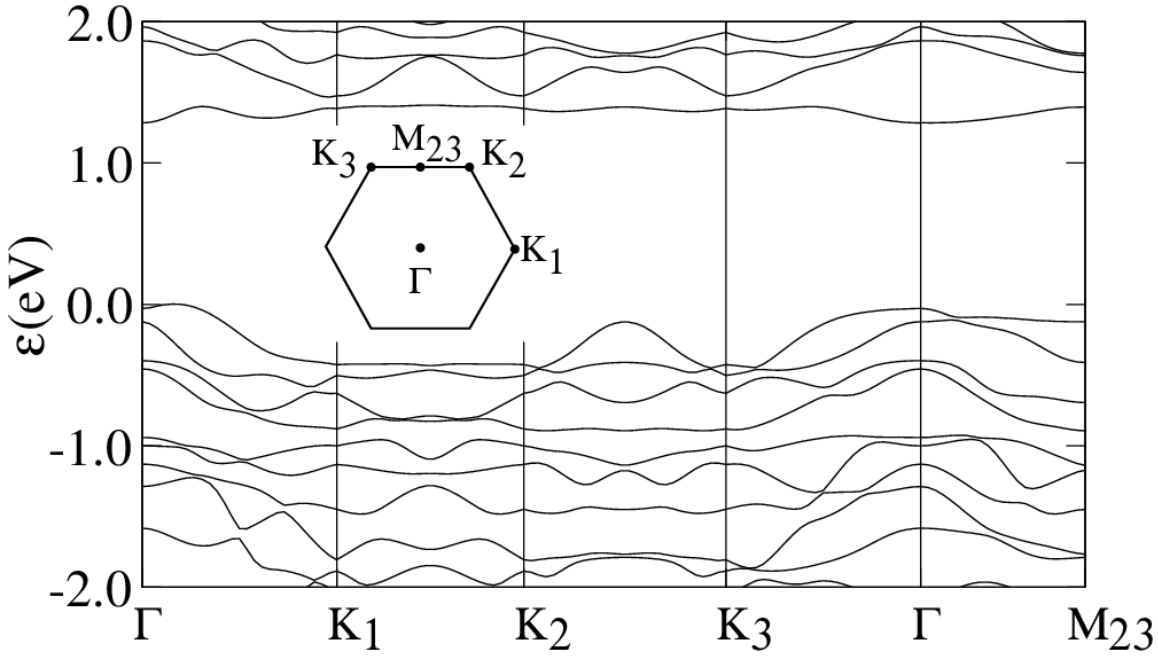

Figure 10. The electronic band structure of monolayer $ReSe_2$ for wavevectors lying in the layer plane as shown in the inset. This calculation used a monoclinic unit cell with a large layer separation and with adjacent layers displaced along the direction of the normal to the layers. This structure generates one reciprocal lattice vector normal to the layer plane, so that the remaining two lie exactly in the layer plane. This emphasizes the approximate symmetry of the near-hexagonal Brillouin zone (see, for example, the near-symmetry which transforms K_2 to K_3 by reflection in the line Γ-M_{23}). For ease of comparison with materials having an exactly hexagonal symmetry, we use the same conventional *k*-point labels K and M here.

Raman signals, (cm^{-1}) 785 nm laser	Raman signals, (cm^{-1}) 532 nm laser	Relative intensity (note, these are angle-dependent)	Calculated Raman-active (A_g) modes (cm^{-1})
-	110.0	not seen	103.6
118	116.7	unresolved	118.0, 123.1
124	123.8	strong	125.9
159	158.2	medium	162.5
174	171.0	medium	175.6
-	179.0	unresolved	179.4, 182.6
193	190.0	medium	194.9
-	194.0	medium	197.7
210	207.7	weak	206.8
219	217.2	weak	219.9
233	231.8	broad	235.1
240	239.0	weak	242.4
248	247.1	weak	251.7
261	260.4	medium	265.8
284	283.6	medium	287.9
-	293.9	weak	298.4

Table 1. Experimental Raman bands observed in bulk and monolayer $ReSe_2$ with two excitation wavelengths, their typical relative strengths, and a summary of the predicted frequencies of the A_g modes calculated by DFPT.

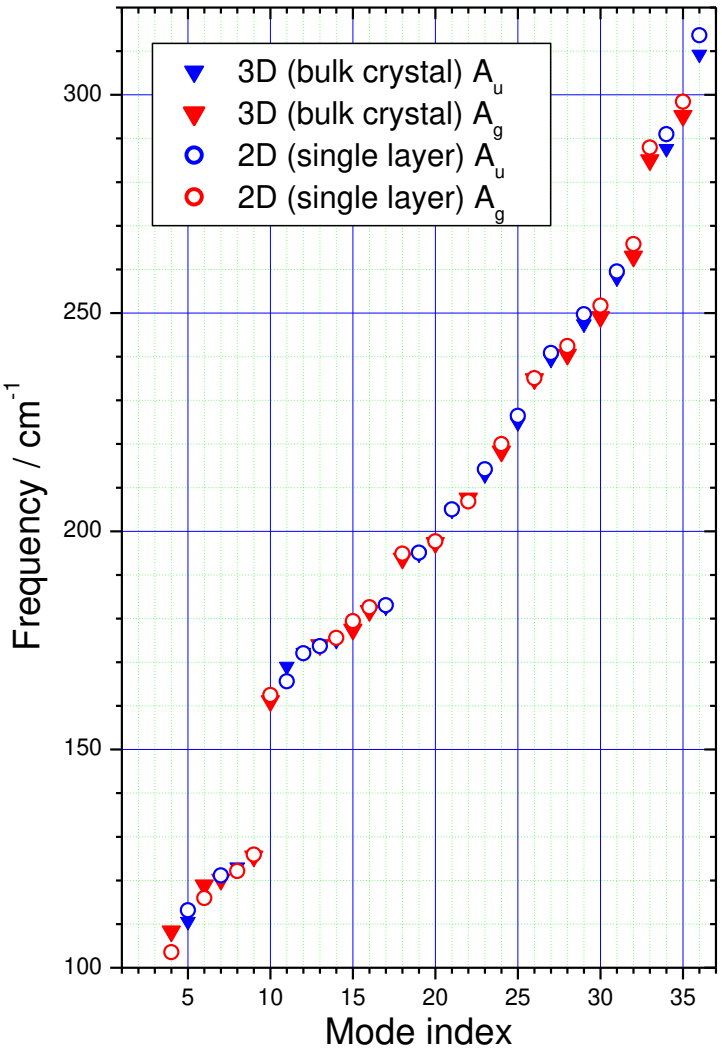

Figure 11. Scatter plot of the vibrational frequencies of the $ReSe_2$ unit cell at the Γ point plotted in order of increasing frequency. Triangles represent modes of the bulk 3D crystal and hollow circles represent modes of a single 2D layer. Raman-active A_g modes are indicated by red symbols and infra-red active A_u modes by blue symbols. This figure emphasizes the fact that our calculations predict no significant change in frequency of the vibrational modes of $ReSe_2$ on reduction of the sample thickness even down to one monolayer.

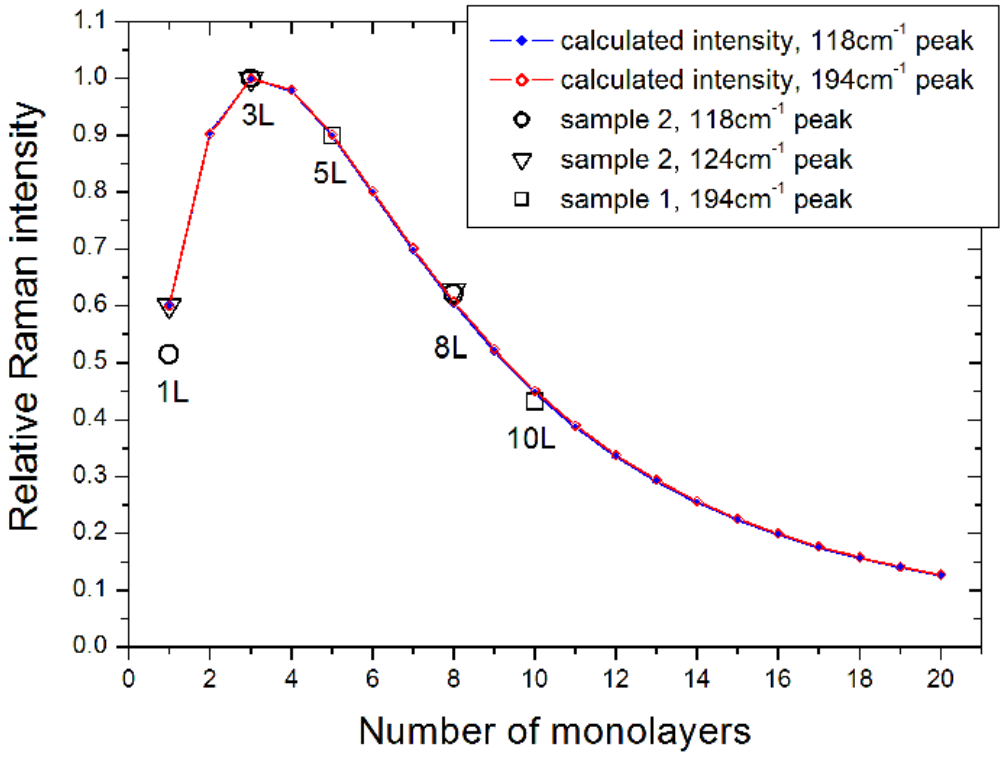

Figure 12. Lines: estimated relative intensities of the 118 and 194 cm^{-1} Raman modes of $ReSe_2$ on a SiO_2 layer thickness of 90 Å with an excitation wavelength of 532 nm as a function of the number of layers. Hollow symbols: experimental data for the two samples discussed in the text. The calculations and data have been normalized to the highest intensity, which occurs for 3L in both calculations and experiment given the present SiO_2 layer thickness. The shape of the curve is not sensitive to the magnitude of the Raman shift, as shown by the overlapping of the two calculated curves. The two data values for sample 1 (squares), which did not contain a 3L flake, have been normalized instead to the predicted 5L intensity and so, for that sample, only the position of the 10L point tests the present model. The calculations were performed according to the model previously applied to MoS_2 and used values of the complex dielectric function typical for the transition metal dichalcogenides (Ref. 53 of the main text) since no experimental data for the dielectric function of $ReSe_2$ is available at present.

Discussion of Figure 12.

It was already shown in Figure 3 that the 5L region of the first sample discussed yields Raman spectra which are about three times *stronger* than those of the 10L region of the same sample. On the other hand, the Raman map of Figure 8(c) shows that the 124 cm^{-1} signal of the 1L region is *weaker* than that of the 3L region, so that the relationship between thickness and Raman signal strength is clearly not monotonic. Therefore, the intensity of any one band will not give an unambiguous measure of layer thickness. Such behavior, arising from interference effects between the Si substrate and the SiO_2 and TMD layers, was noted in graphene[50-52] and was recently analyzed in detail for few-layer TMDs.[53] In that work, it was shown that the ratio of the intensities of the TMD Raman bands to the Si substrate Raman signal varies monotonically and may be used to determine layer thickness.[53] We have applied the analysis of Li *et al*.[53] to estimate the variation in Raman intensity as a function of layer thickness and Raman shift (see Figure 12), and find no significant dependence of the interference effects on Raman shift with the present SiO_2 thickness of 90 nm; all bands are affected equally, with a maximum in the Raman intensity predicted at 3L in agreement with experiment. In these simulations, due to an absence of detailed measurements of the dielectric properties of $ReSe_2$, we have used known values for MoS_2, which is typical of the TMDs investigated by Li *et al*.[53]

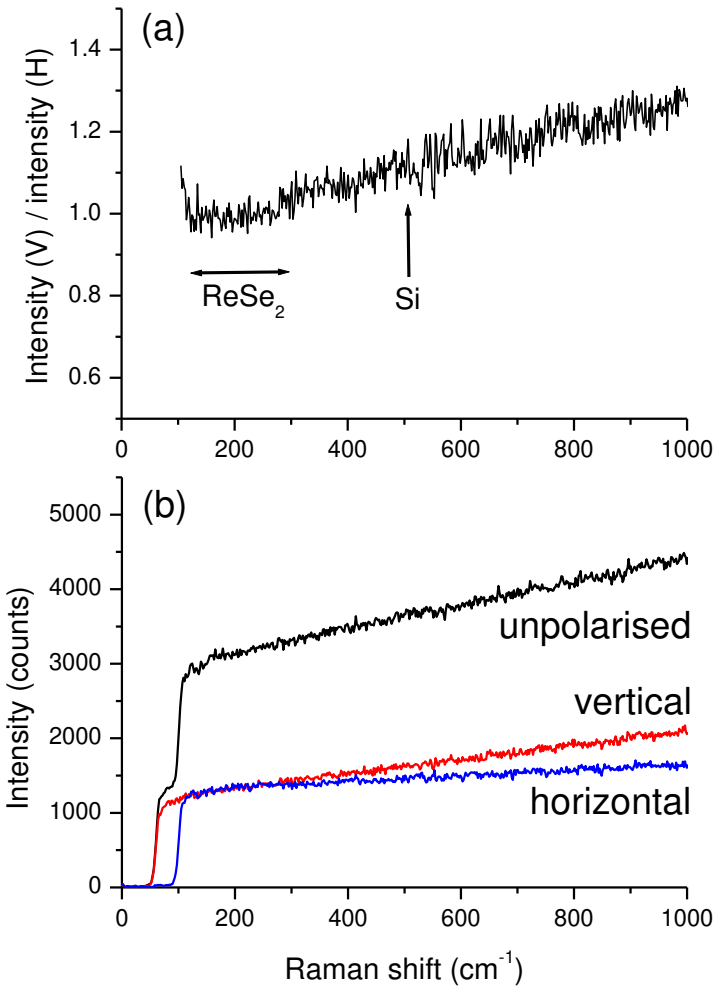

Figure 13. (a) Ratio of the Raman spectrometer response for vertically-polarized (V) white light to that for horizontally-polarized (H) light, where H and V are defined with respect to the laboratory axes. This shows that, over the spectral range of the Raman signals of $ReSe_2$, indicated by the horizontal arrow (100-300 cm^{-1}), the spectrometer is insensitive to the light polarization (the ratio is unity to within about 2%). (b) The spectrometer response for V, H and unpolarized white light separately. This insensitivity to polarization allows us to use the experimental geometries $z(xu)\bar{z}$ and $z(yu)\bar{z}$ in conventional notation without the need to insert a scrambler in the detection beam path. The sharp edge below 100 cm^{-1} is due to the dichroic filters in the system and this is polarization-dependent.

Calculated Raman-active (A_g) frequencies (cm^{-1})	Calculated Raman tensor components (arb. units)		
	u	v	w
103.6	-0.02977	-0.02450	-0.01633
118.0	-0.02626	0.02133	0.08469
123.1	0.01763	0.07145	0.00835
125.9	-0.00286	0.07011	-0.05856
162.5	0.03700	0.01265	0.06836
175.6	-0.03025	-0.00229	0.06864
179.4	0.03076	0.01067	0.08685
182.6	-0.07084	-0.00757	0.04242
194.9	0.06903	-0.01493	-0.00066
197.7	-0.01929	0.02975	0.04967
206.8	0.01460	-0.01852	0.01395
219.9	0.01972	0.07934	0.05550
235.1	-0.16003	0.01347	-0.01448
242.4	0.12859	0.00577	-0.12664
251.7	0.07070	-0.09486	-0.12529
265.8	-0.18443	0.03017	-0.22890
287.9	-0.13467	0.03178	-0.07220
298.4	-0.07461	-0.02985	-0.01608

Table 2. Raman tensor components (as defined by Equation 1 of the main text) of the A_g modes of $ReSe_2$ calculated by DFPT (in this case, using the Quantum Espresso DFPT code and norm-conserving pseudopotentials). Similar results were obtained using the CASTEP DFT code and ultrasoft pseudopotentials.

Equation (2) of the main text gives the scattered intensity $I_T(\theta)$ for a given mode as a function of the Raman tensor parameters u, v and w and the angle θ between the crystal a axis and the incident polarization; for convenience, we repeat Equation (2) here:

$$I_T(\theta) \propto u^2 \cos^2\theta + w^2 \sin^2\theta + v^2 + 2v(u+w)\sin\theta\cos\theta \quad (2)$$

This expression is valid for the case of polarized excitation and unpolarized detection. The angles at which the scattering intensity of that mode has its maximum and minimum values can be found by setting the derivative of the above equation to zero; they are the solutions of

$$\tan 2\theta = \frac{2v}{u-w}. \quad (3)$$

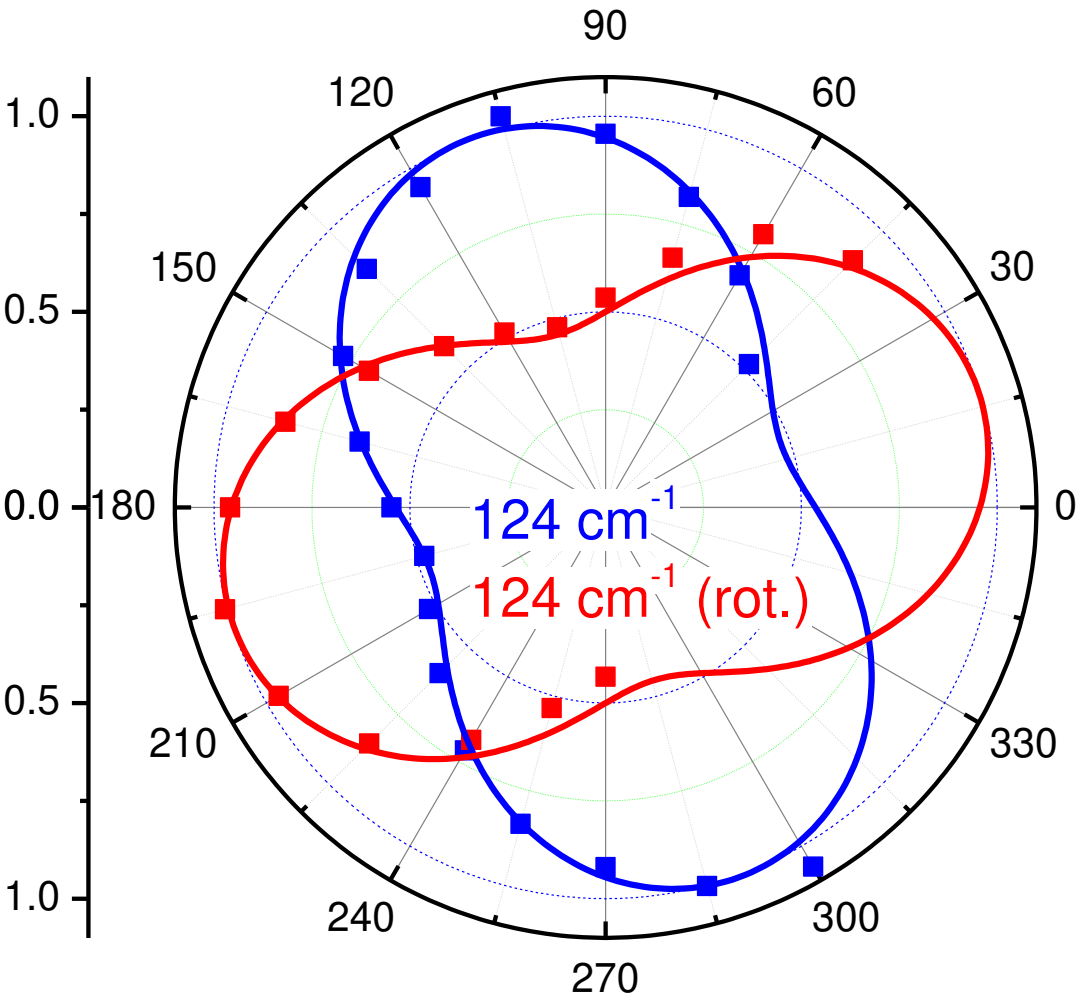

Figure 14. Dependence of the intensity of the 124 cm^{-1} Raman scattering band of $ReSe_2$ on the excitation polarization direction (the zero of angle is the laboratory *x* axis). Squares are data points and solid lines are fits using Equation 2 of the main text. The experiment was carried out before (blue) and after (red) the sample was rotated by 90°. Analysis of the fitted curves shown here according to Equation 3 (this document) shows that the curves are identical apart from a rotation by 90 ± 2°.

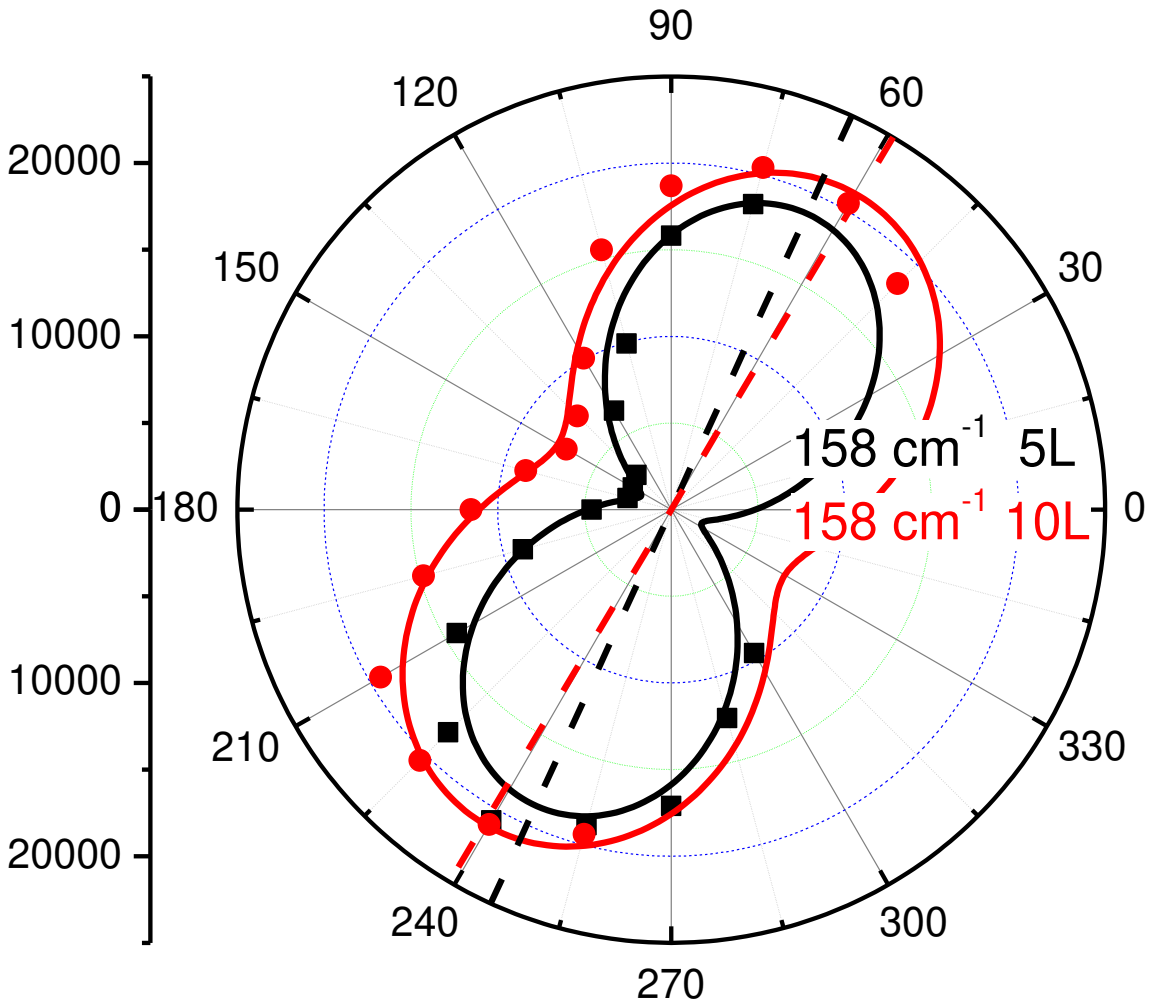

Figure 15. Dependence of the intensity of the 158 cm-1 Raman scattering band of two regions of a single ReSe2 flake on the excitation polarization direction (the zero of angle is again the laboratory x axis). Squares and circles are data points and solid lines are fits using Equation 2 of the main text; the two regions had thicknesses of 5 (black) and 10 (red) monolayers.. Analysis of the fitted curves shown here according to Equation 3 (this document) shows that the curves are displaced by a rotation of 6 ± 2°.